ELSEVIER

Journal of Electroanalytical Chemistry 450 (1998) 175–188

JOURNAL OF ELECTROANALYTICAL CHEMISTRY

The potential of mean force on halide ions near the Cu(100) surface

A. Ignaczak [a], J.A.N.F. Gomes *, S. Romanowski [b]

[a] *CEQUP/Faculdade de Ciências, Universidade do Porto, Rua do Campo Alegre 687, 4150 Porto, Portugal*
[b] *Department of Theoretical Chemistry, University of Lodz, ul. Pomorska 149/153, 90-236 Lodz, Poland*

Received 12 June 1997; received in revised form 25 July 1997

Abstract

This paper reports an investigation of the phenomenon of specific adsorption of halide ions on a Cu(100) surface using Monte Carlo simulations. The system was modeled by considering each ion in a water lamina placed between two copper walls. The potentials used in simulations were constructed by fitting to results of quantum calculations. The solvent contribution to the potential of mean force (pmf) was calculated for each of the four halide ions using the free energy perturbation method. Given the difficulty of finding a reliable ion–metal potential, several alternatives, representing extremal models, were tested in combination with the solvent mean force on the ions, F^-, Cl^-, Br^- or I^-. The results for the pmf on an ion near the metal surface are discussed in the light of the experimental data available. The sensitivity of the results to the type of ion–metal potential used in the simulations is stressed.

Keywords: pmf; Specific adsorption; Halides; Copper surface; Monte Carlo simulation

1. Introduction

The phenomenon of specific adsorption of halide ions on metal surfaces has been a subject of scientific investigation for a long time. Phenomenologically, specific adsorption consists in the chemisorption of ions on an electrode at the point of zero charge as well as in the chemisorption of anions on a negatively charged electrode or cations on a positively charged one, seemingly against the rules of electrostatics in the two latter cases. The mechanism of this phenomenon was investigated in depth using the Green's function method and ECPA (extended coherent potential approximation) [1] for the metal side of the interface.

From the structural point of view the ability of an ion to penetrate into the inner Helmholtz plane (iHp) and to become (or not) adsorbed will depend on its particular properties. Many different experimental techniques (see Refs. [2,3] for review) were used to investigate the properties of the interfacial region and to seek an explanation of the reason why some ions contact adsorb on the electrode surface while the others do not, the halide ions being the most extensively studied. The ion solvation, known to be weaker for ions that adsorb specifically, is assumed to play a decisive role in this phenomenon. However, experimental studies do not give all the necessary information about the interfacial region. In fact, conventional electrochemical techniques [4–6] give a lot of information about the thermodynamics and kinetics of the interfacial processes, but are unable to help with the structural properties. On the other hand, the modern in situ methods produce real-space images of the surface [7–12] but have difficulty in giving insight into the processes occurring there. Spectroscopic techniques were used widely in the last decade to investigate the properties of ions adsorbed on noble metals [13–18]. Unfortunately, most experimental methods are able to investigate the interfacial phenomena only indirectly and, so, an interpretation of results may depend strongly on the initial assumptions.

* Corresponding author. Faculdade de Ciências CEQUP, Universidade do Porto, Praca Gomes Teixeira, 4050 Porto, Portugal. Fax: +351 2 6082959; e-mail: jfgomes@fcl.fc.up.pt

0022-0728/98/$19.00
PII S0022-0728(97)00639-6

Table 1
The parameters used in the V_1 potential for the interaction of halide ions with copper

Parameters	F^-	Cl^-	Br^-	I^-	Units
A_1	181 616.6	187 440.5	181 928.0	339 685.8	kJ mol^{-1}
A_2	4.27018	3.63917	3.38027	3.47876	Å^{-1}
A_3	−222.245	−245.507	−286.910	−217.414	kJ mol^{-1}
A_4	0.69900	0.77313	0.81396	0.76684	Å^{-1}

Though experimental techniques are making rapid progress, many important properties remain unknown. Among them is an exact measurement of all interactions between species involved in the adsorption process, especially those between different phases. Therefore, in recent decades an attempt was made to study interfacial properties using quantum methods. The cluster model was applied to calculate the interaction between the water molecule [19] or the halide ions [20,21] and a metal surface. They provide unique information about pure ion–electrode interaction, that is not available from experiment. These data are necessary for a proper analysis of the forces acting on the ion when it approaches an electrode surface. Thus, results of quantum calculations can be especially useful when combined with statistical techniques which can give a more global description of the interfacial region.

The Monte Carlo (MC) and molecular dynamics (MD) methods have already been applied to the problem of specific adsorption [22–37]. Initially, the interaction of particles with metal surfaces was described only by simple models, neglecting specific properties of the ion and of the metal surface [23–26]. In more recent works this rather limited approximation was substituted by more sophisticated potentials based on quantum calculations, giving a more realistic description of the modeled system [27–29]. Such an approach was used in studies of the free energy of adsorption of ions on Pt(100) [30,31] and on Hg(111) surfaces [32]. These works showed how important structural and thermodynamic information can be obtained from the simulation of systems of this type, but no final clarification of the specific adsorption has been achieved as yet.

In the present work the specific adsorption of halide ions on the copper surface was studied using the MC method. The potentials used in this work are based on quantum calculations [19,21]; however, for the ion–metal, the classical image charge potential is also considered for comparison. The solvent contribution to the potential of mean force (pmf) between each of four halide ions and the Cu(100) surface is presented. Results obtained as a combination of the solvent pmfs with several different models of the ion–metal interaction are shown and discussed.

2. Method

2.1. Metal–ion potentials

In simulations, two different types of ion–metal potentials were tested. The first type is the classical image charge potential in a standard form: $V_{im} = -q_i^2/4(z_m - z_i + W_s)$, where z_m is a z-coordinate of the image plane computed to the center of mass of the system, z_i is the same coordinate for the ion, and W_s is a correction describing the screening due to the electrons on the metal surface. Nevertheless, in a potential defined in this way, the position of the image plane is not very well defined, and is still being discussed in the literature, since it does not consider any structure of the metal side. Therefore, in the present studies, two extremal cases were considered. In one, the image plane is defined by the position of the centres of metal atoms belonging to the first layer (always defined in the next section as $z = {}_0$) and this potential is called V_{im0}. In the second potential, called V_{im}, the position of the image plane is shifted by r_M towards the liquid side, where r_M is the half-diameter of the Cu atom (1.28 Å). Clear limitations of the image charge model are the incorrect description it gives at short distances from the surface and its inability to associate some specificity to the ion.

In the second type of ion–metal potential the chosen function is fitted to results of DFT cluster model calculations [21]. However, also in this case some ambiguity appears due to an unclear interpretation of computed results. If the cluster model used was not big enough to represent the surface, then the values obtained might be significantly underestimated. This yields to the use of a pairwise additive potential, where the interaction with the metal is approximated by an atom–ion potential in the form:

$$V_{X\text{-}Mi} = A_1 \exp(-A_2 r_{X\text{-}Mi}) + A_3 \exp(-A_4 r_{X\text{-}Mi}) \quad (1)$$

where $r_{X\text{-}Mi}$ is the distance from the ion to the ith metal atom, and X = F^-, Cl^-, Br^-, I^-. The total interaction of an ion with a copper wall is then obtained as a summation over all atoms forming the surface:

$$V_1 = \sum_{i=1}^{N} V_{X\text{-}Mi} \quad (2)$$

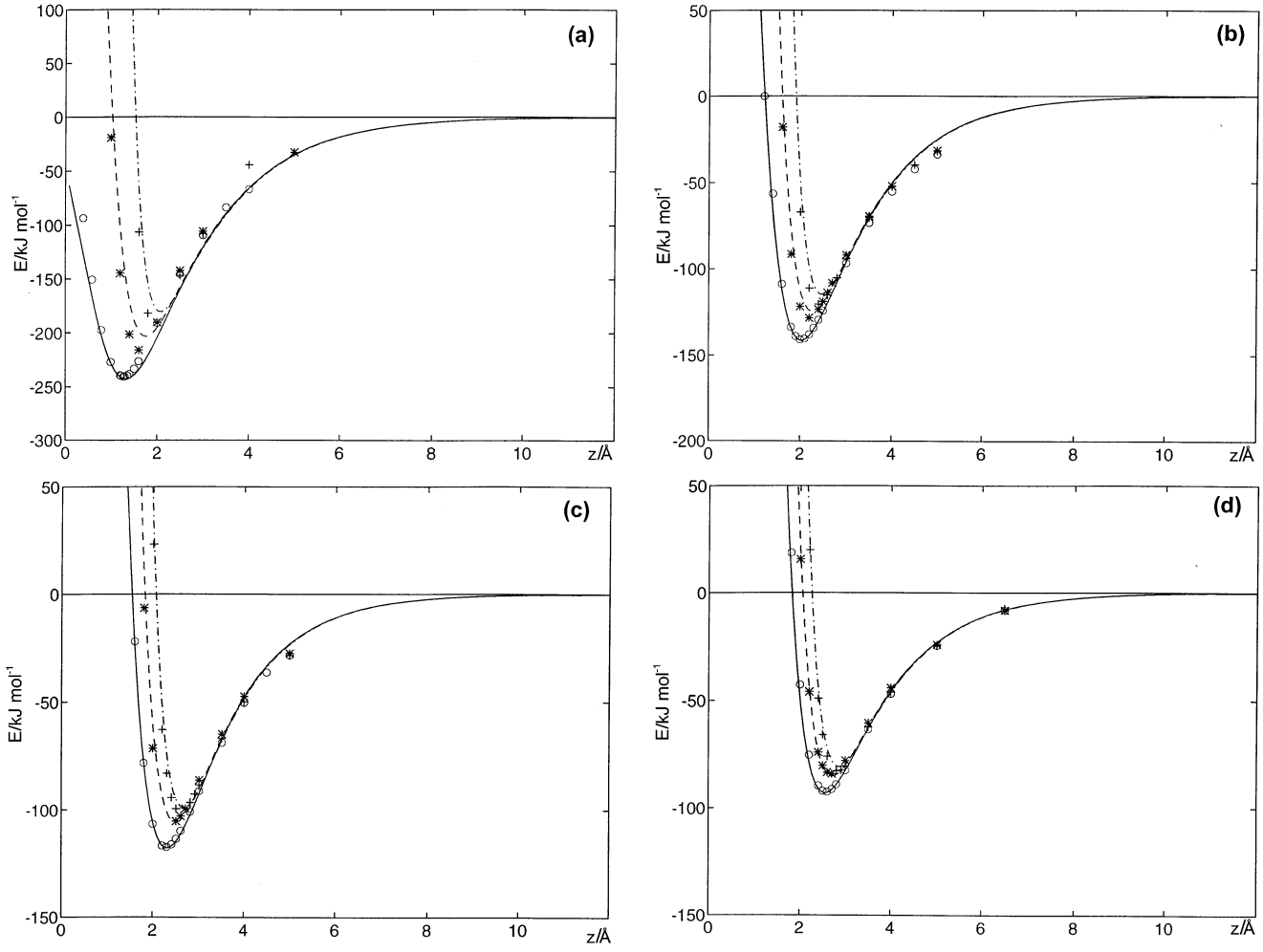

Fig. 1. The behaviour of the halide ion–copper V_1 potential when computed for the Cu_{12} cluster shown together with quantum points to which the potential was fitted. (a) F^-–Cu_{12} interaction, (b) Cl^-–Cu_{12} interaction, (c) Br^-–Cu_{12} interaction, (d) I^-–Cu_{12} interaction. For each ion three positions on the surface are considered, hollow (solid line for analytical potential and (○) for quantum points), bridge (dashed line and (*)) and top (dash-dotted line and (+)).

The parameters $A_1,\ldots,A_4$ obtained from the fitting to the quantum points are given in Table 1. The V_1 potential reconstructs the quantum results when it is summed over the 12 metal atoms forming the cluster used in quantum calculations. This approach has been used in several theoretical works [27–32] on the adsorption of ions on Pt and Hg.

In Fig. 1, the potential V_1 is presented when used for the description of the interaction of the four halide ions with the 12-atom cluster. For evaluation of the quality of the fittings, the quantum calculated points for this cluster are also shown. In Fig. 2 results are shown for this same V_1 potential, but obtained for the interaction of ions with a quasi-infinite wall of metal. As one can see, the interaction described by this potential is indeed much stronger for the infinite wall case, when compared with the 12-atom cluster. However, it is very unclear to what degree distant metal atoms should participate in the total ion–wall interaction and it is likely that this model will grossly overestimate the ion–metal interaction.

Therefore, in the second approach, described by the potential V_2, the total interaction of the ion with the wall is assumed to be well estimated by the interaction energy in the Cu_{12}–X^- cluster. The potential used for description of this interaction was then based on the exponential function of the distance of an ion from the surface:

$$V_0 = B_1 \exp(-B_2 z_X) + B_3 \exp(-B_4 z_X) \quad (3)$$

where the z_X is a distance between an ion and the surface assumed to be at $z = 0$. Then, the corrugation of the surface is introduced to this potential by adding short-range interaction terms as a function of the ion–Cu atom distance:

$$V'_{X\text{-}Mi} = \frac{B_5}{r_{X\text{-}Mi}} \exp(-B_6 r^2_{X\text{-}Mi}) \quad (4)$$

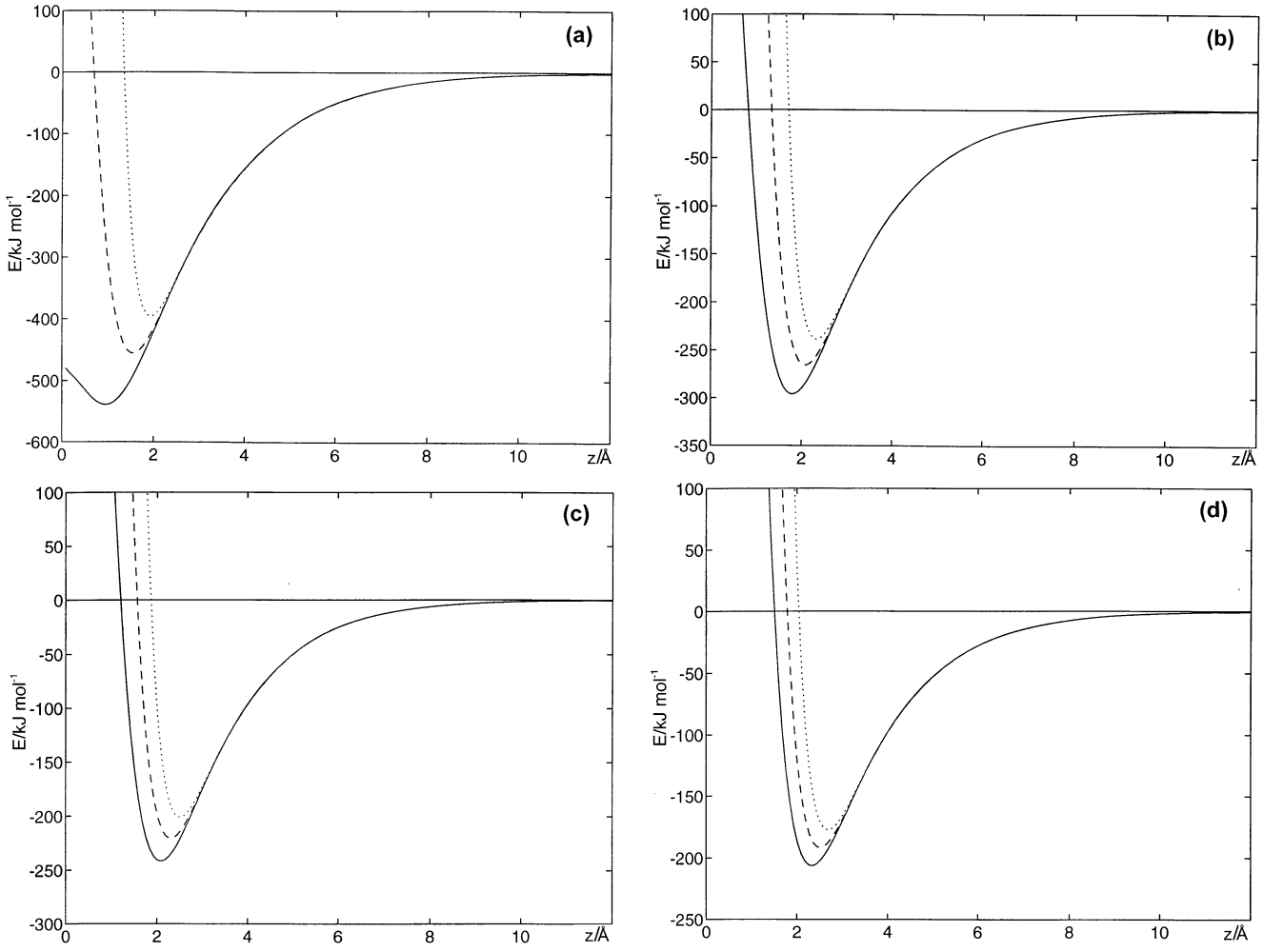

Fig. 2. The ion–copper V_1 potential when computed for the infinite Cu(100) wall case for: (a) F^-, (b) Cl^-, (c) Br^-, (d) I^- (the description of lines is the same as in Fig. 1).

then the total ion–copper interaction is computed as:

$$V_2 = V_0 + \sum_{i=1}^{N} V'_{\text{X-M}i} \quad (5)$$

The parameters obtained from fitting this function to quantum points are given in Table 2. In Fig. 3 the behaviour of the V_2 potential is presented. Since the interaction with the wall is assumed to be the same as that with the 12-atom cluster, the ion–wall V_2 interaction is shown together with quantum points for comparison.

2.2. Ion–water potentials

It has been stressed in several works, that the water–ion interaction probably plays a decisive role in the specific adsorption process. The energy cost for the reorientation of the H_2O molecule to its less favoured positions is much bigger for fluoride than for the three other ions, and may be important when changes occur in the first hydration shell of the ion. Therefore an attempt has been made to find a simple potential that would model not only the most stable orientation of the water molecule, but also other less preferred conformations.

To construct the potential energy surface of the halide ion–water interaction, a set of standard HF calculations was performed. The basis sets used for halide ions were the same as in the calculations of the metal–ion interaction, namely full double-zeta (DZ) quality description of F^- [38], while for larger ions Wadt and Hay pseudopotentials were used for core electrons and the DZ basis sets for valence electrons [39]. For the water molecule, the 6-31G basis set was extended by adding polarization functions. For two smaller ions, the counterpoise correction was found to be necessary to reconstruct the experimentally known interaction energies [40]. For each ion–water case, eight different orientations of the water monomer towards the ion have been studied computing the interaction energy at various distances. The attractive ion–water orientations were favoured, the most stable being found

Table 2
The parameters used in the V_2 potential for the interaction of halide ions with copper

Parameters	F^-	Cl^-	Br^-	I^-	Units
B_1	173 249.77	204 784.04	220 617.24	319 681.52	kJ mol^{-1}
B_2	0.97804	1.01350	1.04436	1.03333	Å^{-1}
B_3	−173 264.84	−204 115.71	−219 554.67	−318 312.40	kJ mol^{-1}
B_4	0.97418	1.00914	1.03960	1.03000	Å^{-1}
B_5	12 619.72	12 716.61	12 949.12	15 967.54	kJ mol^{-1} Å
B_6	1.60415	1.08939	0.93684	0.85005	Å^{-2}

from the optimization of the distance between species and of the angle between the dipole moment of the H_2O monomer and the ion–oxygen axis. The calculated energy minimum for the preferred orientations of water is in agreement with experimental data on the four ions. All calculations were performed using the GAUSSIAN92 program [41].

A new potential was constructed using the function proposed by Nguyen et al. [42], but modified with an orientational exponential term applied to the oxygen part of the function. The final form of this modified potential is:

$$V_{XW} = V_{X-O} + V_{X-H1} + V_{X-H2} \tag{6}$$

where:

$$\begin{aligned} V_{X\text{-}O} &= \frac{D_1}{r_{X\text{-}O}} + \frac{D_2}{r_{X\text{-}O}^2} f_{or} + D_3 \exp(-D_4 r_{X\text{-}O}) \\ V_{X\text{-}H1} &= \frac{D_5}{r_{X\text{-}H1}} + \frac{D_6}{r_{X\text{-}H1}^2} + D_7 \exp(-D_8 r_{X\text{-}H1}) \\ V_{X\text{-}H2} &= \frac{D_5}{r_{X\text{-}H2}} + \frac{D_6}{r_{X\text{-}H2}^2} + D_7 \exp(-D_8 r_{X\text{-}H2}) \\ f_{or} &= \exp(-D_9 |r_{X\text{-}H1} - r_{X\text{-}H2}|) \end{aligned} \tag{7}$$

This potential was fitted to quantum points for each ion–water system and the parameters are given in Table 3. The quality of the fittings of this potential to the quantum points for four halide ions can be seen in Fig. 4. The new potential proposed in this work describes the change of the ion–water interaction energy when the H_2O monomer is forced to take an orientation less preferred in close agreement to the quantum points. It should be stressed that this potential was tested for each halide ion by simulations of the gas-phase $X^-(H_2O)_n$ cluster formation as well as of the ionic solution at infinite dilution. The structural and thermodynamic properties of the systems were found to be in good agreement with experimental data available.

2.3. Metal–water and water–water potentials

The water–Cu(100) potential was taken to be the same as was used in the MC simulations of the liquid water between two metal walls [43]. This potential was built by fitting the parameters of the analytical function to recent results obtained from the B3LYP simulations [19]. It has an additive form where each water–metal atom interaction is described by the function:

$$V_{W\text{-}Mi} = V_{O\text{-}Mi} + V_{H1\text{-}Mi} + V_{H2\text{-}Mi} \tag{8}$$

where:

$$\begin{aligned} V_{O\text{-}Mi} &= [C_1 \exp(-C_2 r_{O\text{-}Mi}) \\ &\quad + C_3 \exp(-C_4 r_{O\text{-}Mi})][1 - f(\rho_i)] + C_6 \exp(C_7 r_{O\text{-}Mi}) \\ f(\rho_i) &= \exp\left(-C_5(\rho_i - \frac{a}{2})^2\right) \end{aligned}$$

$$\begin{aligned} V_{H1\text{-}Mi} &= C_8 \exp(-C_9 r_{H1\text{-}Mi}) + C_{10} \exp(-C_{11} r_{H1\text{-}Mi}) \\ V_{H2\text{-}Mi} &= C_8 \exp(-C_9 r_{H2\text{-}Mi}) + C_{10} \exp(-C_{11} r_{H2\text{-}Mi}) \end{aligned} \tag{9}$$

The variables $r_{O\text{-}Mi}$, $r_{H1\text{-}Mi}$ and $r_{H2\text{-}Mi}$ are the distances of the Cu atom to, respectively, the oxygen and the hydrogens of the water molecule; the ρ_i variable is a projection of the oxygen to metal atom vector onto the surface; a is the metal lattice constant for copper, equal to 3.6077 Å. The function $f(\rho_i)$ is introduced to force the bridge and top positions on the surface to be preferred for water adsorption, as predicted by the results of DFT calculations. Additionally, each $V_{W\text{-}M}$ term is multiplied by the function $f_s = 1/(1 + \exp(\beta(r_{O\text{-}Mi} - \lambda)))$ to switch it smoothly to zero for longer atom–molecule distances to avoid an artificial increase in the water–copper interaction when the 12-atom cluster is substituted by a much larger structure mimicking the infinite wall. The parameters for the water–copper potential obtained by fitting the potential to quantum points are presented in Table 4.

The interaction of the H_2O monomer with the Cu(100) wall described by this potential for several orientations and sites on the surface is shown in Fig. 5. The interaction with a wall has the minimum energy of 35.5 kJ mol^{-1} at the bridge site, in agreement with experimental estimates of this value. The properties of

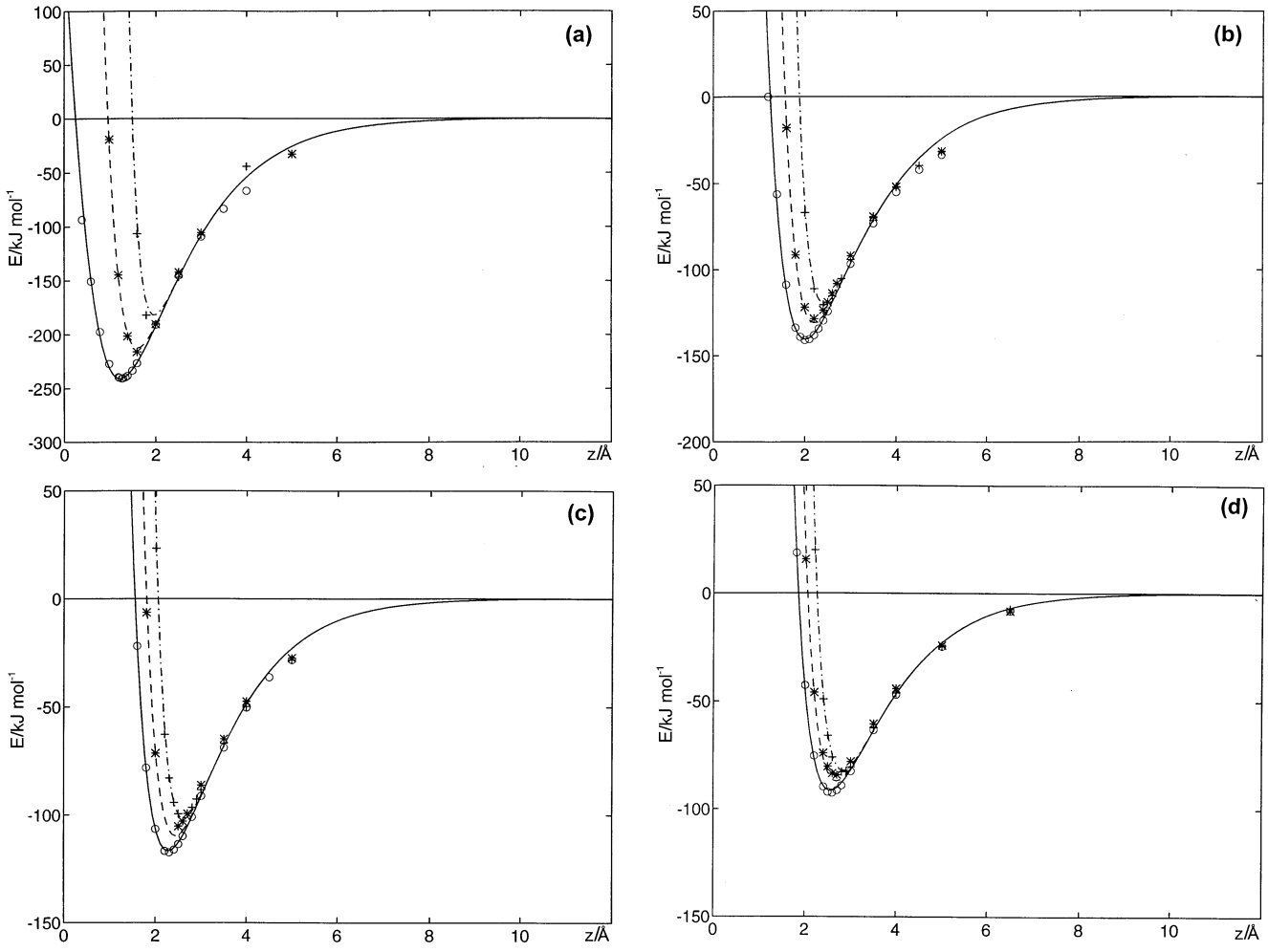

Fig. 3. The ion–copper V_2 potential when computed for the infinite Cu(100) wall case for: (a) F^-, (b) Cl^-, (c) Br^-, (d) I^- (the same description of analytical potential and quantum points as in Fig. 1)

the electrode|electrolyte interface were found to be sufficiently well described by this potential in MC simulations. Fig. 6 shows a structure formed by the first layer of waters on the Cu(100) surface as predicted by this model. In a detailed examination, some six-sided rings typical for ice-like structures may be found, but some four- and five-sided rings are also present. This distribution is such that no clear pattern appears. Most water molecules lie parallel to the metal surface, but another orientation, with an O–H bond parallel to the surface and the other in a perpendicular plane, is also common. The structure of the first layer may be said to be determined by the tendency of the liquid to preserve hydrogen bonds but the metal–water interaction has some influence on it.

For the description of the water–water interaction the TIP4P model of water [44] was used. This is a rigid, four-points model, with an experimental length of O–H bonds of 0.9572 Å, and a dipole moment of 2.18 D. The positive charges of 0.52 are located on hydrogens, while a negative charge is located on a point shifted by 0.15 Å from the position of the oxygen atom along the symmetry axis of the H_2O molecule towards hydrogens. The TIP4P model has been used in many simulations of processes occurring in aqueous solutions and proved to describe sufficiently well properties of bulk water.

2.4. Simulations

The simulations of aqueous solutions in contact with Cu(100) were carried out at a temperature of 298.15 K on the NVT ensemble. The simulation box in the calculations is the same as was used previously in studies of properties of liquid water in contact with a Cu(100) surface [43]. In the present studies, 255 water molecules and one ion were placed between two metal walls, each one measuring about 18 Å in the x and y directions, and located at a distance of about 12.2 Å from the center mass of the system. The metal sides of the box are modeled by two slabs, each one consisting

Table 3
The parameters used in the V_{xw} potential for the interaction of halide ions with water

Parameters	F^-	Cl^-	Br^-	I^-	Units
D_1	704.1135	760.3519	958.6041	1025.2908	kJ mol^{-1} Å
D_2	330.4578	325.6342	290.2396	411.8697	kJ mol^{-1} Å^2
D_3	460 175.8	722 270.3	2 445 293	10 385 638	kJ mol^{-1}
D_4	4.024856	3.59914	3.992442	4.5426120	Å^{-1}
D_5	−342.905	−365.413	−458.196	−497.578	Å kJ mol^{-1}
D_6	−192.204	−220.199	−269.925	−287.061	Å^2 kJ mol^{-1}
D_7	13 184.99	11 915.11	8668.997	12 828.13	kJ mol^{-1}
D_8	4.006362	2.920188	2.392718	2.2870791	Å^{-1}
D_9	0.674246	0.637145	0.362145	0.2301453	Å^{-1}

of 300 Cu atoms arranged in a typical fcc crystallographic structure. In the directions parallel to the metal surface the periodic boundary conditions were applied.

To study the specific adsorption phenomenon of halide ions on the copper surface, the potential of mean force (pmf) between each halide ion in aqueous solution and the Cu(100) surface was calculated. To compute the solvent averaged mean force acting on the ion the free energy perturbation method (FEP) [45,46] was used. For each ion, the following procedure was applied: first the ion was fixed in the bulk, at a certain distance from the metal surface. In each window, the initial position was always above the hollow site that is preferred for the adsorption of halides on the metal surface. Then, a run ('window') consisting of an equilibration phase of 3.5×10^6 configurations and a production phase of 2.5×10^6 configurations was used to compute the free energy difference dA_i between perturbed and reference system. During this latter phase of the run an ion was allowed to move in the x and y directions, while it was sequentially perturbed by $\pm$ 0.15 Å in the z direction (for fluoride, at distances closer to the surface, the perturbation step was decreased to 0.1 Å due to larger dA_i differences). Next, the ion was dragged along the z-axis towards the wall by 0.3 Å and the same equilibration and sampling procedure was repeated for the new window. In the perturbation method the doublewide sampling method was used, where the free energy difference $A(z_i + dz) - A(z_i)$ and $A(z_i - dz) - A(z_i)$ are obtained in one simulation. The pmf profile of A^s versus distance of the ion to the surface is then obtained by the successive summation of dA_i. To test the validity of the results, another method of calculating pmf was used simultaneously, where the solvent force on the ion was computed directly from the derivative of the ion–water potential in each window, and then the averaged mean force was integrated from the state of an ion in the bulk to the given distance from the surface. However, since the results were very close (a discrepancy of not more than 4 kJ mol^{-1} was found between the values obtained with the two methods) only the results obtained with the FEP method are shown in this paper.

3. Results

The calculated solvent contribution A^s to the potential of mean force for adsorption of halide ions is displayed in Fig. 7. The Cu(100) wall on the picture is located on the left side, while the right side is expected to model the bulk-like conditions. Indeed the A^s at distances far from the surface is approximately equal to zero, manifesting a symmetric (in statistical average) environment. In this region the solvent pmf profile for all ions behaves rather smoothly, showing only flat descent at distances of about 7–8 Å. This effect, appearing to some extent for all ions, could be due to the interference of the hydration shell of the ion with the second hydration layer of the metal. In this region, the orientation of waters in this layer agrees approximately with the orientation of waters in the first hydration shell of the ion, i.e. with hydrogens pointing away from the metal surface. For all ions, a closer approach to the metal wall causes repulsion, but the distance at which an increase of A^s occurs depends on the type of ion. As might be expected from the size of the ions and of their solvation shells, and from the magnitude of the solute–solvent interaction energies that run in the reverse order, there is a region where the pmf curves cross and exchange positions. Therefore, while the solvent pmf for iodide is the most repulsive at a distance of about 4.5–5 Å, it finally becomes the smallest at the optimal z-distance predicted for its contact adsorption on the metal. This finding disagrees with results of MD simulations of Spohr [32] where the pmf of halide ions adsorbing on mercury were studied. In this latter work it was found that the repulsion on chloride is definitely smaller than that on iodide for ion–metal distances of less than 6 Å. In the present study the ordering of solvent pmfs on the ions contact adsorbed on the metal is rather close to what might be predicted from the hydration enthalpies of halide ions. This tendency is

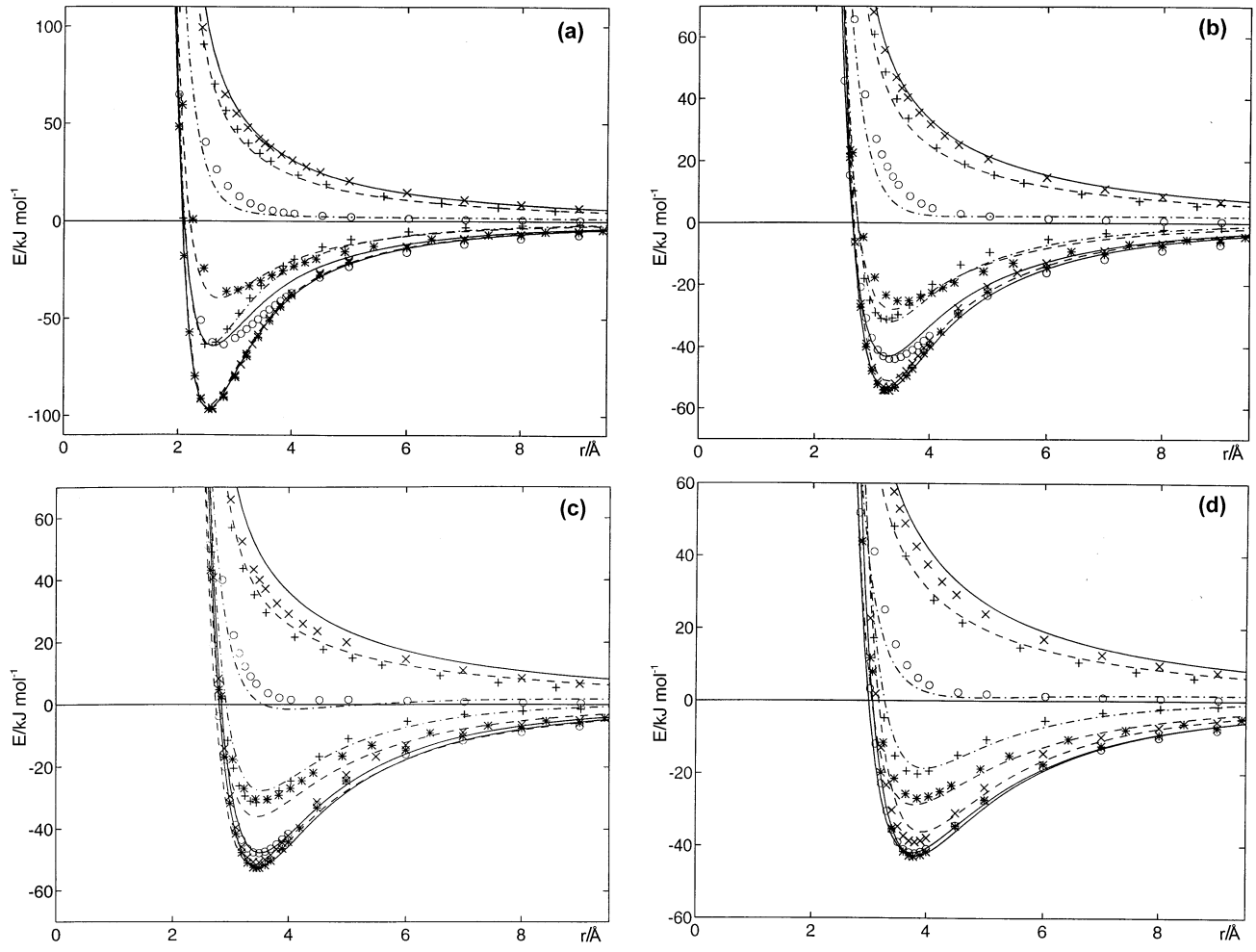

Fig. 4. The $X^- - H_2O$ potential (solid, dashed and dash-dotted lines) shown together with quantum points (○,*, ×, +) for several different orientations of water molecules towards the halide ion: (a) F^-, (b) Cl^-, (c) Br^-, (d) I^-. Orientations are defined by angles: α (the angle of the dipole moment of water with the $O–X^-$ axis) and β where necessary (the angle between the H–H axis with the $O–X^-$ axis): (solid line, *) α = optimal; (dashed line, ×) $\alpha = 52.26°$ (X–H–O linearly situated); (solid line, ○) $\alpha = 0°$; (dash-dotted line, +) $\alpha = 90°$ and $\beta = 0°$; (dashed line, *) $\alpha = 45°$ and $\beta = 90°$ (hydrogens towards the ion); (dash-dotted line, ○) $\alpha = 90°$ and $\beta = 90°$; (dashed line, +) $\alpha = 135°$ and $\beta = 90°$ (oxygen towards the ion); (solid line, ×) $\alpha = 180°$ and $\beta = 90°$.

easily seen for fluoride and iodide, while for bromide and chloride a somewhat unclear situation can be noticed in Fig. 7. The solvent mean force for bromide seems to have slightly larger values than for chloride, but both curves run very closely, as should be expected from the relatively small difference between the hydration enthalpies for the two ions. Nevertheless, when the steric effect is considered, the A^s results for chloride and bromide at their optimal distance from the surface do appear to be in the right order (see an explanation below).

The distances at which pmf, A^s, for larger ions become repulsive are very close to values which can be obtained by summing the radius of the first hydration shell of each ion (defined by the maximum of RDF_O) with the position of the first hydration layer of the metal (as read from the maximum of the oxygen density profile). This crude estimation gives ion–metal distances of about 4.85, 5.50, 5.75 and 6.05 Å for F^-, Cl^-, Br^- and I^-, respectively. Thus, our free energy calculations seem to confirm that up to these distances the three larger ions are able to approach the Cu(100) surface without significant changes in their hydration shells. For fluoride, the solvent pmf curve has a somewhat different shape. In this case a weak repulsion on the ion is observed already at a distance of about 6.5 Å and the A^s is kept at approximately constant level up to about 4.7 Å. It may be assumed that the first hydration shell of F^- is slightly modified already when it passes the second hydration shell of the metal. The sharp increase in the repulsion on fluoride occurs for distances of less than 4.5 Å due to the stronger reorganization of waters, when the range of the hydration shell of the ion reaches the region forbidden for water adsorption on the metal surface.

For the optimal ion–surface distances as computed from the quantum calculations [21], pmf A^s values were

found of about 300 kJ mol^{-1} for F^-, 126 kJ mol^{-1} for Cl^-, 122 kJ mol^{-1} for Br^- and 97 kJ mol^{-1} for I^-. As can be seen, the solvent mean force values at these positions follow the same order as the hydration enthalpies. In all cases these values are approximately equivalent, energetically, to losing about two to three water molecules from the first hydration shell of the ion. This feature of the ion solvation under adsorption on the Cu(100) surface agrees quite well with results for fluoride and iodide adsorbed on Pt(100) and Hg(111) surfaces [32]. However, unlike that reported in studies of the Hg(111) surface, no particular stabilization of fluoride at the distance between the second and the first hydration layer of the Cu(100) surface was found; nevertheless, in this range of distances the behaviour of fluoride differs from the other ions.

To obtain the total pmf profiles, the solvent contribution of pmf on each ion was combined with different models of the ion–metal potential, as described in the previous section. In Fig. 8 the pmf, A^s, curves for all four ions are combined with two extremal cases of image charge potential. It is obvious that using the image charge model for the description of the ion–metal interaction, one cannot obtain proper characteristics for the region where an ion is expected to be contact adsorbed, since for short distances this coulomb type potential has no minimum but tends to $-\infty$. From Fig. 8 it can be seen that the position of the image plane is in fact crucial for the quality of the final results. The pmf_{im} profiles (dashed lines), obtained as a combination of V_{im} potential with A^s, for all ions show very similar behaviour. No meaningful minimum is found on any curve, neither in the range of the outer Helmholtz plane (oHp) nor of the inner Helmholtz plane (iHp). Of course, in this latter case the total pmf cannot have a minimum, since the infinite values of the image potential will always dominate results for A^s in the region close to the metal surface. The importance of the correct definition of the position of the image plane can be seen when pmf_{im} results are compared with pmf_{im0} curves that are drawn in the same figure by solid lines. There are some very important differences between curves for the four halide ions. The pmf_{im0} profiles for the three larger ions are definitely smoother than that obtained for fluoride. All curves do have some minimum at a distance that might be identified as an approximate position of oHp for each ion. When an ion comes closer to the surface, some energetic barrier is found in this model for all ions. This barrier is found to be the largest for fluoride adsorption and much smaller for the three other ions. For very short distances of the ions to the surface, the image potential dominates the solvent pmf and the contact adsorption is assumed to occur in this region. This general picture is in good qualitative agreement with electrochemical experiments which report much stronger adsorption of Cl^-, Br^- and I^-, and none or only very weak adsorption of F^-.

Table 4
The parameters used in the $V_{W\text{-}M}$ potential for the interaction of water molecule with copper

Parameter	Values	units
C_1	5 159 633.6	kJ mol^{-1}
C_2	3.69587	Å^{-1}
C_3	−4 777 387.4	kJ mol^{-1}
C_4	3.64781	Å^{-1}
C_5	2.97950	Å^{-2}
C_6	44 576.24	kJ mol^{-1}
C_7	3.27578	Å^{-1}
C_8	141 259.91	kJ mol^{-1}
C_9	1.81080	Å^{-1}
C_{10}	−137 904.31	kJ mol^{-1}
C_{11}	1.80132	Å^{-1}
β	2.0	Å^{-1}
λ	4.0	Å

However, this must be examined in more detail, especially in the region close to the surface. Experimental estimates from the in situ X-ray reflectivity measurements of the ion–metal interlayer spacing for larger halides adsorbed on gold suggest this to be about 2.4 ± 0.3 Å for the three larger ions [13–15]; smaller values should be then expected for the case of copper due to the smaller radius of the Cu atom. The optimal distances found for the Cu(100) surface in DFT cluster calculations range from 1.3 Å for F^-, to 2.0 Å for Cl^-, 2.3 Å for Br^- and 2.6 Å for I^-. Now, it may be seen in Fig. 8 that the potential of mean force pmf_{im0} profile predicts all ions to suffer some repulsion at these distances before being strongly attracted at shorter distances. The region of contact adsorption of ions is then predicted for extremely short distances, at which image potentials are known to be incorrect.

In Fig. 9, the total pmf is shown as obtained from the combination of A^s with analytical potentials V_1 and V_2, these being two alternative approaches to using the results of cluster calculations. Since in each window of the simulations the ion was found to stay close to the initial position, i.e. on the perpendicular of the hollow site of the surface, the A^s values were combined with energy values for the interaction of the ion with copper at this site. As expected, the pmf profiles are significantly different from those presented in Fig. 8 in the close neighbourhood of the surface. These new potentials describe the ion–metal interaction in a more realistic way, but because of their extremal character, manifested in very different energy values, the total pmf_{V_1} and pmf_{V_2} do not have similar shape. The V_1 potential seems to overestimate strongly the ion–metal interaction. In all cases only one minimum is exhibited by the pmf_{V_1} (dashed lines in Fig. 9), located in the iHp and all ions in this model are assumed to be specifically adsorbed without any local stabilization state in the

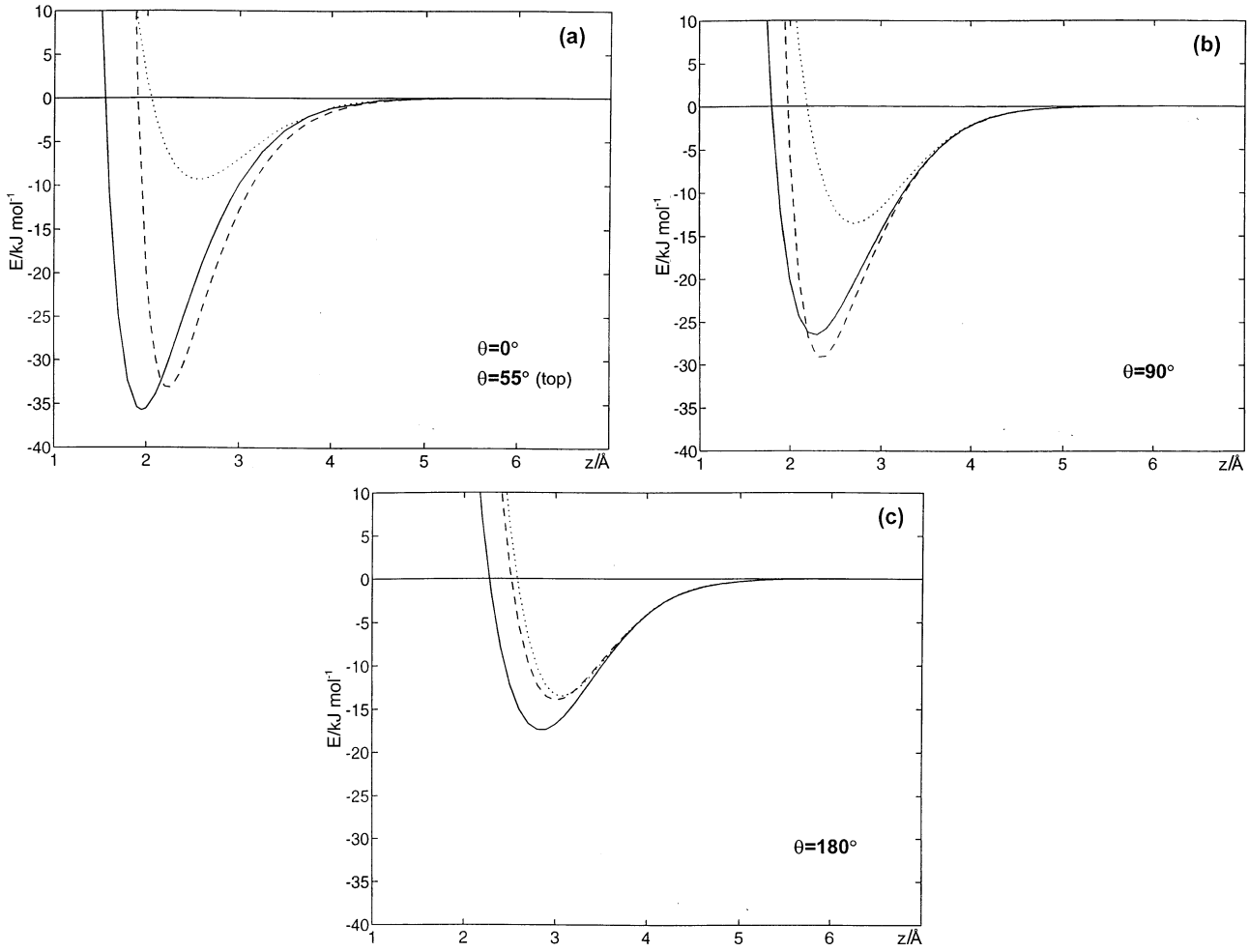

Fig. 5. The behaviour of the water–copper potential when computed for the quasi-infinite Cu(100) wall for different orientations of H_2O molecule: (a) with an oxygen pointing towards the surface; (b) with the H_2O plane parallel to the surface; (c) with the oxygen pointing away from the surface and the molecular plane of water perpendicular to it. For each orientation three sites on the surface were tested: top (dashed line), bridge (solid line) and hollow (dotted line). In (a) at the bridge and hollow sites the orientation of the water is perpendicular to the surface, while at the top site the tilt angle, θ, between the dipole moment of water and the normal to the surface is 55°.

region of oHp. Very similar results for F^- and I^- adsorption on Hg were found from MD simulations of Spohr [32], where a pairwise additive potential based on cluster model calculations was also used for the ion–mercury interaction. Although some evaluation of the cluster size effect on computed values was done in this latter work, it is well known that the cluster model, independently of its size, is always a very poor representation of an infinite metal surface, and may contain artificial effects coming from the specific properties of the cluster used. The cluster size effect on the energy values is difficult to predict and the comparison based on just two different sized clusters as was made for mercury may not be enough for a proper evaluation. For this reason we considered two extremal cases of different descriptions of the ion–copper interactions, believing that the correct behaviour will be somewhere in between.

In the last potential that was tested, V_2, the ion–Cu(100) interaction is assumed to be equal to that found for the 12-atom cluster calculations. The pmf_{V_2} curves (represented in Fig. 9 by a solid line for each ion) show behaviour extremely different from that of pmf_{V_1}. While in the previous case all ions were found to adsorb on the surface, the pmf_{V_2} predicts the occurrence of non-specific adsorption, i.e. for each ion it has some minimum around a distance of 5.5–6 Å that is the oHp region. When the ion comes closer to the surface, the mean force becomes slightly repulsive and it finds some small energetic barrier. The largest difference is seen for the closest distance from the surface. For the three larger ions the pmf_{V_2} shows some kind of local minimum, very shallow and not very well defined, but located at distances close (shifted towards the larger values by about 0.3 Å) to the optimal positions predicted for ions, at 2.4 Å for Cl^-, at 2.7 Å for Br^- and at 3.0 Å for I^-, in the latter case being very weakly marked. The difference between positions of the first and the second pmf_{V_2} minimum is in all cases about 3 Å, which is close to the

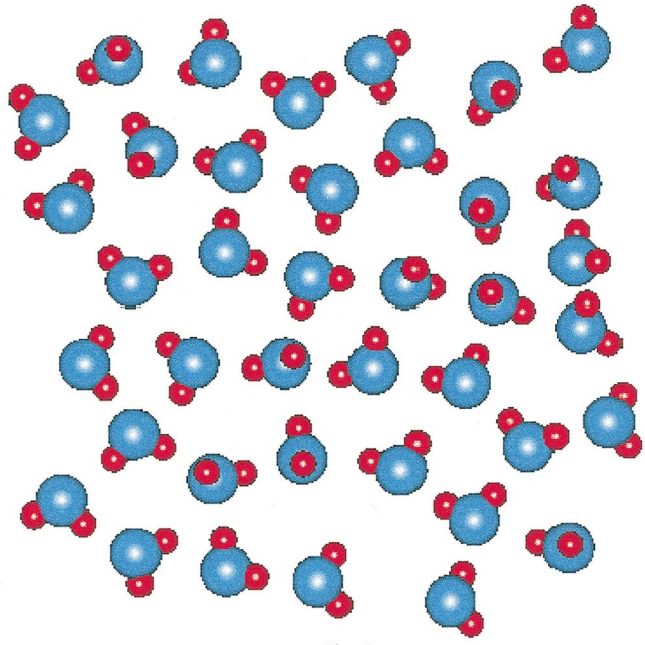

Fig. 6

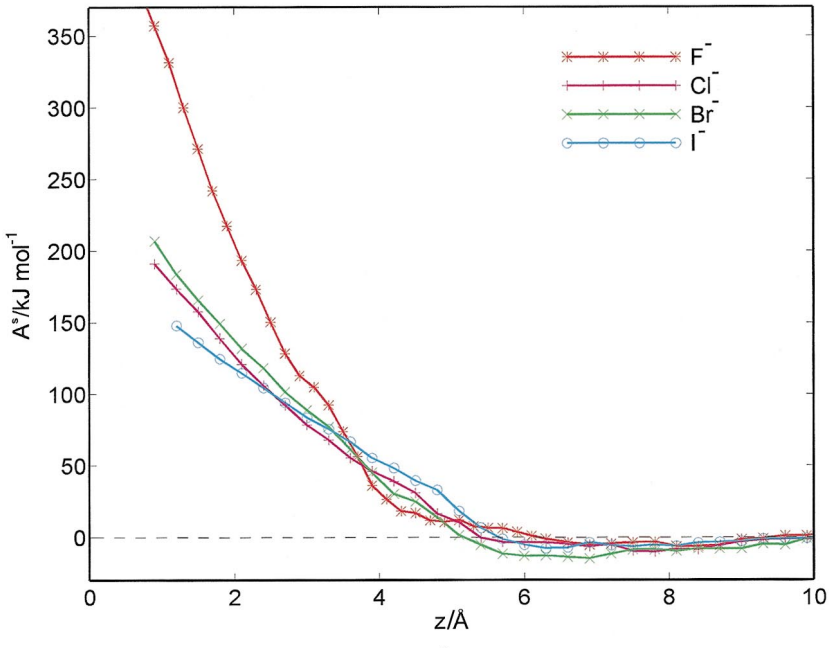

Fig. 7

Fig. 6. The distribution of waters on the Cu(100) surface taken from the last configuration obtained in the simulation of 256 water molecules between the two copper walls.

Fig. 7. The solvent mean force A^s acting on each of the four halide ions near the Cu(100) surface.

radius of the hydration shell of the halide ion. For fluoride, due to its smaller size, the first minimum related to the non-specific adsorption state is at about 4.5 Å and is slightly deeper than for the other ions. At the same time the second minimum expected at about 1.3 Å is not present on the pmf_{V_2} curve for F^-. This agrees qualitatively with experimental predictions, that fluoride is adsorbed non-specifically, while the other ions can contact adsorb. However, at the same time, the pmf_{V_2} curves have generally repulsive character and even for the larger ions the specific adsorption is unlikely to occur due to the shallowness of the well.

The comparison of all pmf results obtained with different models of ion–metal potential shows how important it is to use a correct definition of this interaction. Even a slight change in the ion–metal potential

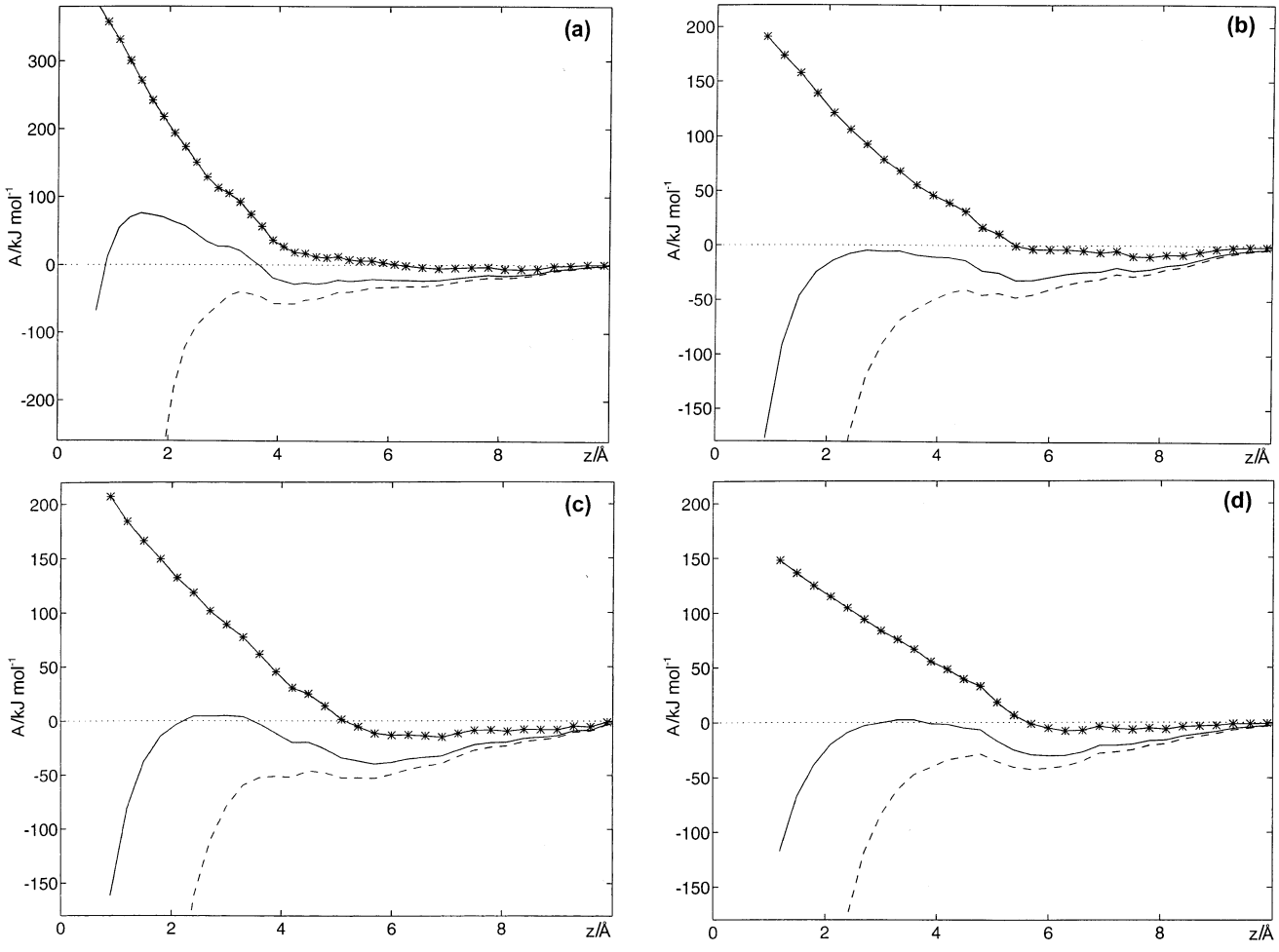

Fig. 8. The pmf of (a) F^-, (b) Cl^-, (c) Br^-, (d) I^- obtained for each ion as a combination of solvent pmf A^s with the image charge potentials: V_{im} (dashed line) and V_{im0} (solid line). For each ion the solvent contribution to the potential of mean force is also shown (-*-).

may have a great influence on the total force on the ion near the surface, and thus for the true description of the specific adsorption phenomenon it seems to be crucial to know exactly the strength and the range of the interaction of the ion with the metal.

4. Conclusions

Given the complexity of the experimental systems where specific adsorption is observed, the model used here may be considered oversimplified. The two slabs of metal that represent the electrodes are assumed to be rigid and to have no net charge; the electrolyte solution is represented by pure water plus one halide ion, without any other ionic species. However simple, this model allows the estimation of the two components of the forces acting upon the ion, that are normally thought to be determinant of the specific adsorption, namely the direct interaction between the metal and the ion and the average force exerted by the water on the ion. The most important result reported here is the solvent contribution to the pmf on the four halide ions as estimated from Monte Carlo simulations. Very few studies of this type have been published, considering only Pt(100) and Hg(111). The present results may be said to agree qualitatively with the solvent pmfs reported for F^- and I^-, but not with those for Cl^-. In fact, the magnitude of the solvent mean force on the halide ions in the iHp region as reported here follows the trend of the ion–water interaction, while chloride did appear to behave differently in earlier publications [32]. To the best of our knowledge, there are no previous results for bromide.

The global picture of the adsorption process cannot be studied without a detailed knowledge of the ion–metal interaction. From the results of the present work it appears that both models—the classical image potential as well as the potential based on quantum calculations—provide the correct description of the interfacial region only in some limited range of the ion–surface distances. The image charge potential is shown to be

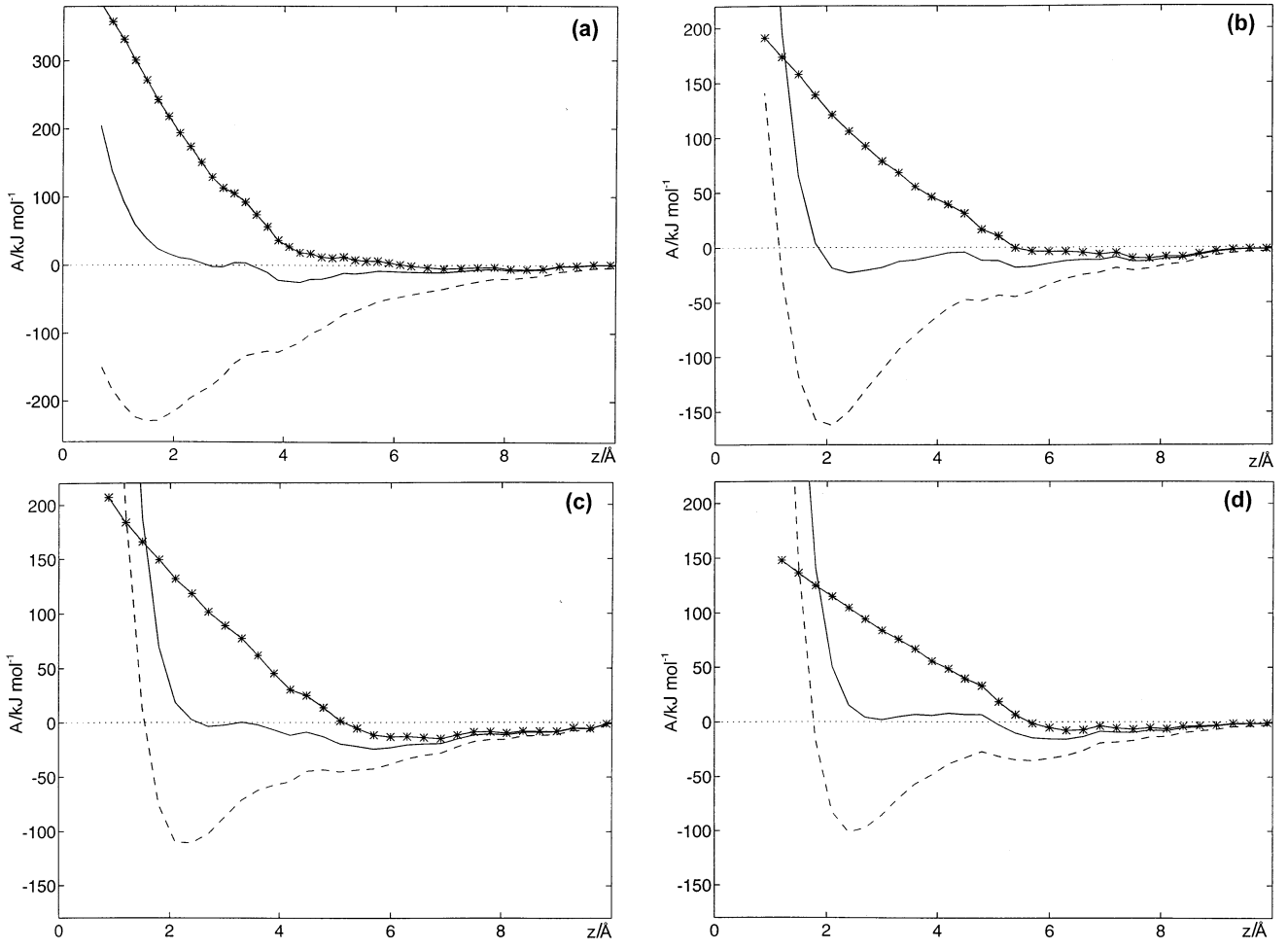

Fig. 9. The total pmf obtained from the combination of A^s with analytical potentials: V_1 (dashed line) and V_2 (solid line) for each halide ion: (a) F^-, (b) Cl^-, (c) Br^-, (d) I^-. The pmf A^s on each ion is also included (-*-).

appropriate for the region distant from the metal. The analytical potential based on quantum calculations gives a realistic description of the ion–metal interaction at a distance close to the energy minimum, but is likely to be incorrect at longer distances. None of them is totally adequate for the description of the most important region, i.e. the range of distances where the solvated ion coming to the surface starts to modify its hydration shell, but is not yet contact adsorbed on the metal. The choice of potential was found to be crucial for the quality of the final results. The two tested potentials, V_{im} and V_1, do clearly overestimate short-range ion–metal interaction. In both cases, the ordering of the total free energy of adsorption is opposite to that reported experimentally [4]. Even considering the extremely different conditions of experimental and theoretical investigations (such as the concentration of ions in solutions and the presence of the other ions, usually counterions) the prediction of a much stronger adsorption of F^- at infinite dilution, when compared to the other halide ions, is unlikely to be correct.

For the two other potentials, V_{im0} and V_2, it was found that when an ion comes to the surface, it must go through some energy barrier to be contact adsorbed on the electrode. For both types of potential this barrier was found to be much larger for fluoride than for the other three halide ions. The pmf_{V_2} profiles show qualitatively two possible states of adsorption—in the oHp and in the iHp—as predicted experimentally.

Acknowledgements

We gratefully thank Professor W. Schmickler for helpful discussions. The financial support of JNICT (Lisbon) is acknowledged. A.I. thanks PRAXIS XXI for a doctoral scholarship.

References

[1] S. Romanowski, Polish J. Chem. (and references therein) 67 (1993) 729.

[2] A. Hamelin, T. Vitanov, E. Sevastyanov, A. Popov, J. Electroanal. Chem. 145 (1983) 225.
[3] R. Parsons, Chem. Rev. 90 (1990) 813.
[4] D. Larkin, K.L. Guyer, J.T. Hupp, M.J. Weaver, J. Electroanal. Chem. 138 (1982) 401.
[5] J.O'M. Bockris, M. Gamboa-Aldeco, M. Szklarczyk, J. Electroanal. Chem. 339 (1992) 355.
[6] H.D. Hurwitz, A. Jenard, B. Bicamumpaka, W. Schmickler, J. Electroanal. Chem. 349 (1993) 49.
[7] X. Gao, M.J. Weaver, J. Am. Chem. Soc. 114 (1992) 8544.
[8] W. Haiss, J.K. Sass, X. Gao, M.J. Weaver, Surf. Sci. Lett. 274 (1992) L593.
[9] X. Gao, G.J. Edens, M.J. Weaver, J. Phys. Chem. 98 (1994) 8074.
[10] X. Gao, G.J. Edens, F.C. Liu, A. Hamelin, M.J. Weaver, J. Phys. Chem. 98 (1994) 8086.
[11] X. Gao, M.J. Weaver, Ber. Bunsenges. Phys. Chem. 97 (1993) 507.
[12] D.W. Suggs, A.J. Bard, J. Phys. Chem. 99 (1995) 8349.
[13] J. Wang, B.M. Ocko, A.J. Davenport, H.S. Isaacs, Phys. Rev. B46 (1992) 10321.
[14] B.M. Ocko, G.M. Watson, J. Wang, J. Phys. Chem. 98 (1994) 897.
[15] O.M. Magnussen, B.M. Ocko, R.R. Adzic, J.X. Wang, Phys. Rev. B51 (1995) 5510.
[16] P. Gao, M.J. Weather, J. Phys. Chem. 90 (1986) 4057.
[17] B. Pettinger, M.R. Philpott, J.G. Gordon II, J. Phys. Chem. 85 (1981) 2746.
[18] G. Niaura, A. Malinauskas, Chem. Phys. Lett. 207 (1993) 455.
[19] A. Ignaczak, J.A.N.F. Gomes, J. Electroanal. Chem. (and references therein) 420 (1997) 209.
[20] A. Ignaczak, J.A.N.F. Gomes, Chem. Phys. Lett. 257 (1996) 609.
[21] A. Ignaczak, J.A.N.F. Gomes, J. Electroanal. Chem. (and references therein) 420 (1997) 71.
[22] D.A. Rose, I. Benjamin, J. Chem. Phys. 95 (1991) 6856.
[23] D.A. Rose, I. Benjamin, J. Chem. Phys. 98 (1992) 2283.
[24] J.N. Glosli, M.R. Philpott, J. Chem. Phys. 96 (1992) 6962.
[25] J.N. Glosli, M.R. Philpott, J. Chem. Phys. 98 (1993) 9995.
[26] J.N. Glosli, M.R. Philpott, Electrochim. Acta 41 (1996) 2145.
[27] J. Seitz-Beywl, M. Poxleitner, K. Heinzinger, Naturforsch. Z. 46a (1991) 876.
[28] G. Tóth, K. Heinzinger, Chem. Phys. Lett. 245 (1995) 49.
[29] E. Spohr, G. Tóth, K. Heinzinger, Electrochim. Acta 41 (1996) 2131.
[30] L. Perrera, M.L. Berkowitz, J. Phys. Chem. 97 (1993) 13803.
[31] E. Spohr, Chem. Phys. Lett. 207 (1993) 214.
[32] E. Spohr, Acta Chem. Scand. 49 (1995) 189.
[33] R.R. Nazmutdinov, E. Spohr, J. Phys. Chem. 98 (1994) 5956.
[34] A.R. Newmark, W. Schmickler, J. Electroanal. Chem. 329 (1992) 159.
[35] O. Pecina, W. Schmickler, E. Spohr, J. Electroanal. Chem. 394 (1995) 29.
[36] O. Pecina, W. Schmickler, E. Spohr, J. Electroanal. Chem. 405 (1996) 239.
[37] W. Schmickler, Electrochim. Acta 41 (1996) 2329.
[38] T.H. Dunning, P.J. Hay, Modern Theoretical Chemistry, ch. 1, Plenum, New York, 1976, pp. 1–28.
[39] W.R. Wadt, P.J. Hay, J. Chem. Phys. 82 (1985) 284.
[40] M. Arshadi, R. Yamdagni, P. Kebarle, J. Phys. Chem. 74 (1970) 1475.
[41] M.J. Frisch, G.W. Trucks, H.B. Schlegel, P.M.W. Gill, B.G. Johnson, M.W. Wong, J.B. Foresman, M.A. Robb, M. Head-Gordon, E.S. Reprogle, R. Gomperts, J.L. Andres, K. Ragchavachari, J.S. Binkley, C. Gonzales, R.L. Martin, D.J. Fox, D.J. DeFrees, J. Baker, J.P. Stewart J.A. Pople, GAUSSIAN 92/DFT, Revision F.2, Gaussian Inc., Pittsburgh, PA, 1993.
[42] H.L. Nguyen, S.A. Adelman, J. Chem. Phys. 81 (1984) 4564.
[43] A. Ignaczak, J.A.N.F. Gomes, submitted for publication.
[44] W.L. Jorgensen, J. Chandrasekhar, J. Madura, R.W. Impey, M.L. Klein, J. Chem. Phys. 79 (1983) 926.
[45] R.W. Zwanzig, J. Chem. Phys. 22 (1954) 1420.
[46] W.L. Jorgensen, J.K. Buckner, S.E. Huston, P.J. Rossky, J. Am. Chem. Soc. 109 (1987) 1891.